The effect of pressure on vibrational modes in Li_3PO_4

2002 J. Phys.: Condens. Matter 14 461

(http://iopscience.iop.org/0953-8984/14/3/314)

INSTITUTE OF PHYSICS PUBLISHING JOURNAL OF PHYSICS: CONDENSED MATTER

J. Phys.: Condens. Matter **14** (2002) 461–469 PII: S0953-8984(02)29165-1

The effect of pressure on vibrational modes in Li_3PO_4

Randy J Smith, Yongrong Shen and Kevin L Bray

Department of Chemistry, Washington State University, Pullman, WA 99164-4630, USA

Received 26 September 2001, in final form 20 November 2001
Published 21 December 2001
Online at stacks.iop.org/JPhysCM/14/461

Abstract

We have studied the effect of pressure on the stretching and bending modes of $(PO_4)^{3-}$ molecular groups in undoped Li_3PO_4 and $(MnO_4)^{3-}$ groups in Mn^{5+}-doped Li_3PO_4 using Raman spectroscopy and luminescence. The high-pressure Raman spectroscopy study confirmed an irreversible phase transition from the high-temperature phase to the low-temperature phase, observed in our previous high-pressure luminescence study (Riedener T, Shen Y R, Smith R J and Bray K L 2000 *Chem. Phys. Lett.* **321** 445) and further characterized the rate and irreversibility of the phase transition. We observed and analysed vibronic transitions occurring in the ^1E emission of Mn^{5+} in both phases. A stronger vibronic transition associated with the bending mode is interpreted in terms of an $E \otimes e$ Jahn–Teller coupling. Bulk and local compressibilities were predicted from variations of the energies of the $(PO_4)^{3-}$ and $(MnO_4)^{3-}$ stretching modes with pressure.

1. Introduction

For the past decade, great attention has been paid to materials activated with $3d^2$ transition metal ions (e.g., Cr^{4+}, Mn^{5+}, and Fe^{6+}) because of their applicability as tunable solid-state lasers in the near-infrared (NIR) range. There have appeared numerous studies of the spectroscopy [1–11], electron spin resonance [12–14], and high-pressure luminescence spectroscopy [15–19] of the $3d^2$-activated materials.

The intensity and bandwidth of the vibronic luminescence of Cr^{4+} in host lattices are decisive factors that govern the tunability, wavelength, and efficiency of NIR lasers. Our recent high-pressure luminescence studies of Cr^{4+} in forsterite (Mg_2SiO_4) [17] and in yttrium silicate (Y_2SiO_5) [18] revealed that non-tetrahedral distortions significantly influence the electronic structure and the electron–vibrational coupling of $3d^2$ ions and, as a consequence, these distortions govern the luminescence properties of $3d^2$-activated materials.

Mn^{5+} is a useful diagnostic of the properties of $3d^2$ ions because of the fine spectral structure of its $^1E \leftrightarrow {}^3A_2$ transitions. This fine spectral structure permits Mn^{5+} to be used as a probe of local distortions and electron–vibrational coupling. We successfully used the high-pressure luminescence properties of a Mn^{5+} dopant as a probe of a phase transition of Li_3PO_4 [19].

0953-8984/02/030461+09$30.00

Li_3PO_4 is well known to exist in a dimorphic form. Li_3PO_4 possesses a high-temperature phase (HTP) and a low-temperature phase (LTP) [20, 21]. The structure is orthorhombic for both phases and the space group is $Pnma$ for the LTP and $Pmn2_1$ for the HTP. The cell volume in the HTP is ∼1.4% larger than in the LTP. Li^+ and P^{5+} are tetrahedrally coordinated by oxygen anions in both phases of Li_3PO_4. The P–O bond lengths are very similar in the two phases (averages: 1.546(7) Å in the LTP and 1.555(20) Å in the HTP) and the O–P–O angles deviate slightly from the regular tetrahedral value (109.5°), with an average deviation of ∼0.7° in the LTP and of ∼0.5° in the HTP [20, 21]. Keffer *et al* [21] observed a temperature-induced LTP → HTP phase transition at ∼502 °C. In our previous study [19], we induced the reverse HTP → LTP phase transition at pressures above ∼120 kbar.

The purpose of our present work is to use high-pressure Raman and luminescence spectroscopy to systematically study the effect of pressure on the vibrational modes and the electron–vibrational coupling in undoped and Mn^{5+}-doped Li_3PO_4. Our objective is to correlate the variations of the vibrations with the luminescence properties of $3d^2$ ions through the electron–vibrational coupling. The dimorphic Li_3PO_4 system possesses two structures, a slightly distorted HTP structure and a more distorted LTP structure, with similar chemical features and provides a unique opportunity to gain a deeper understanding of local distortions and electron–vibrational coupling effects in $3d^2$ systems.

2. Experimental procedure

Undoped and 0.1% Mn^{5+}-doped HTP Li_3PO_4 single crystals were provided by Professor Hans U Güdel at the University of Bern. Undoped LTP Li_3PO_4 powder was commercially available and was purchased from Aldrich.

High pressure was generated by a gasketed Merrill-Bassett diamond-anvil cell (DAC). The sample was placed in the DAC inside a hole (200 μm in diameter) of an Inconel gasket. Pressure was determined by the standard ruby luminescence technique and with a linear shift (0.365 Å $kbar^{-1}$) of the ruby R_1 line [22]. A 4:1 methanol:ethanol mixture or a spectroscopic polydimethyl siloxane oil served as the pressure-transmitting medium in room temperature high-pressure Raman scattering experiments. In low-temperature high-pressure luminescence experiments, the 4:1 methanol:ethanol mixture only served as the pressure-transmitting medium because of its known hydrostatic pressure distribution at low temperatures [22] and each pressurization was always carried out at room temperature in order to maintain the hydrostatic pressure distribution when the DAC was cooled. The two pressure media used for the room temperature high-pressure Raman spectroscopy showed no significant difference—not only in the pressure dependence of the line positions and shapes of Raman lines but also in the transition pressure for Li_3PO_4 of interest in this study.

Raman scattering measurements were performed using a micro-Raman spectroscopy set-up. The set-up consisted of an Ar^+ laser (Coherent 52), a microscope (Nikon MM-40), a 0.55 m monochromator (Spex Triax 550), and a CCD detector (Princeton Instruments 1152EM/1). The 514.5 nm Ar^+ laser line was employed as the excitation source. The laser line was reflected by a 514.5 nm holographic beam splitter into the microscope, and focused onto the sample in the DAC (∼5 μm in laser beam size). The scattered light was first filtered by a 514.5 nm super-notch holographic filter and was focused onto the entrance slit (100 μm in slit width) of the monochromator.

NIR luminescence measurements were performed with a continuous-wave spectroscopy set-up. Luminescence was excited with an excitation wavelength of ∼600 nm from a dye laser (Spectra-Physics 375B; rhodamine 590) pumped by a 7 W Ar^+ laser multilines (Lexel 95), dispersed with a 1 m monochromator (Spex 1704/2), and detected with a Ge

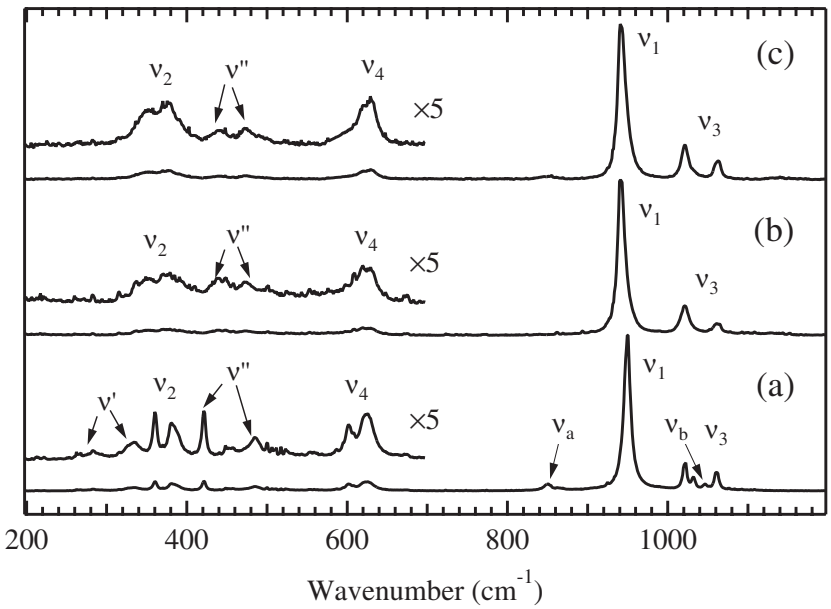

Figure 1. Room temperature Raman spectra of bulk HTP Li_3PO_4 crystal (a) and LTP Li_3PO_4 powder (b) as well as Li_3PO_4 crystal (c) obtained by decompressing down to ambient pressure. All Raman spectra were normalized to their ν_1-mode intensity. The ν'- and ν''-labelled Raman peaks are the lattice modes. The ν_a- and ν_b-labelled Raman peaks are overtones of $\nu_2(360\ \mathrm{cm}^{-1}) + \nu''(490\ \mathrm{cm}^{-1})$ and $\nu''(421\ \mathrm{cm}^{-1}) + \nu_4(626\ \mathrm{cm}^{-1})$, respectively.

Table 1. Ambient-pressure vibrational modes (cm^{-1}) for $(PO_4)^{3-}$ and $(MnO_4)^{3-}$. Free-ion modes are taken from [23].

	$\nu_1(a_1)$ (cm^{-1})	$\nu_2(e)$ (cm^{-1})	$\nu_3(t_2)$ (cm^{-1})	$\nu_4(t_2)$ (cm^{-1})
$(PO_4)^{3-}$ (free)	938	420	1017	567
$(PO_4)^{3-}$ (HTP)	950	360, 381	1022, 1032, 1061	602, 624
$(PO_4)^{3-}$ (LTP)	942	352, 377	1022, 1063	600, 625
$(MnO_4)^{3-}$ (free)	810	324	838	349
$(MnO_4)^{3-}$ (HTP)	800	333, 341	—	487, 538
$(MnO_4)^{3-}$ (LTP)	800	313, 318	—	428, 490

detector (ADC 403UL) using a standard lock-in technique. Low temperature was achieved by mounting the DAC on a closed-cycle helium cryostat (APD Cryogenics).

3. Raman spectroscopy

Figure 1 shows ambient-pressure Raman spectra of HTP Li_3PO_4 crystal (figure 1(a)) and LTP Li_3PO_4 powder (figure 1(b)) at room temperature. The HTP and LTP Li_3PO_4 samples exhibited similar features in the Raman spectrum. The spectra consisted of four groups of vibrational modes (labelled by $\nu_i, i = 1$–4). The ambient-pressure energies of the ν_i-modes in both phases are presented in table 1.

In an undistorted tetrahedron (T_d symmetry), the molecular vibrations are composed of two stretching modes ($\nu_1(a_1)$ and $\nu_3(t_2)$) and two bending modes ($\nu_2(e)$ and $\nu_4(t_2)$), all of

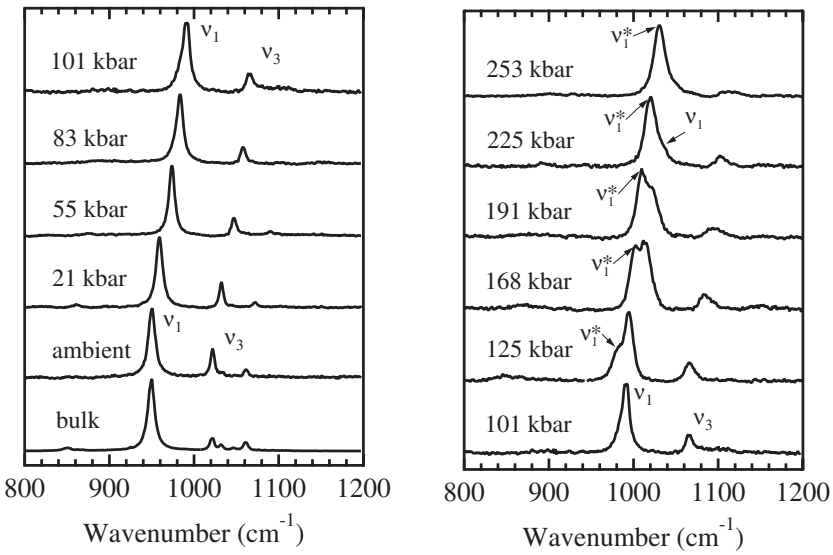

Figure 2. Representative room temperature Raman spectra of HTP Li_3PO_4 crystal at several pressures. All spectra were normalized to the most intense peak.

which are Raman active. The site symmetry of $(PO_4)^{3-}$ in the HTP and LTP Li_3PO_4 systems is slightly distorted from a regular tetrahedron to a formal C_s site symmetry [20, 21]. The tetrahedral vibrational modes will therefore split and we can formally expect three sub-bands ($2a' + a''$) from a threefold-degenerate T_d mode (ν_3 or ν_4) and two sub-bands ($a' + a''$) from a twofold-degenerate T_d mode (ν_2). In our present study, however, for convenience and because the distortions are slight, a tetrahedral approximation will be used to describe the observed Raman peaks.

From figures 1(a) and (b), we see that the stretching modes ($\nu_{1,3}$) are stronger than the bending modes ($\nu_{2,4}$). Moreover, the stretching mode (ν_1) is dominant in intensity and appears 8 cm^{-1} higher in energy in HTP Li_3PO_4 (950 cm^{-1}) than in LTP Li_3PO_4 (942 cm^{-1}).

For high-pressure Raman spectroscopy studies, we primarily focused on the stretching modes ($\nu_{1,3}$) because of their higher Raman intensity. Figure 2 shows representative room temperature Raman spectra of Li_3PO_4 under pressure up to 253 kbar. We began by pressurizing the HTP Li_3PO_4 up to ∼120 kbar and found a monotonic blue-shift of the $\nu_{1,3}$-modes with pressure. Upon further compression, a new Raman peak (labelled ν_1^*) appeared on the lower-energy side of the HTP ν_1-mode and gradually gained in intensity. A simultaneous gradual decrease in the HTP ν_1-mode intensity was also observed. As pressure was increased above ∼225 kbar, the HTP ν_1-mode disappeared completely.

Upon release of pressure, the ν_1^*-mode shifted to the red and remained observable in the fully released, ambient-pressure state. No HTP modes returned. A detailed ambient-pressure Raman spectrum of the depressed Li_3PO_4 crystal is shown in figure 1(c), and is identical to the Raman spectrum of the LTP Li_3PO_4 powder (figure 1(b)). We therefore conclude that pressure induces an irreversible phase transition from the HTP to the LTP as observed in our previous luminescence studies of Mn^{5+}:Li_3PO_4 [19].

Repeated runs of the high-pressure Raman spectroscopy experiment indicated that the pressure-induced HTP → LTP phase transition began at ∼120 kbar and finished at ∼230 kbar. The phase transition process is very slow and a transition rate of ∼0.9% per kbar was determined

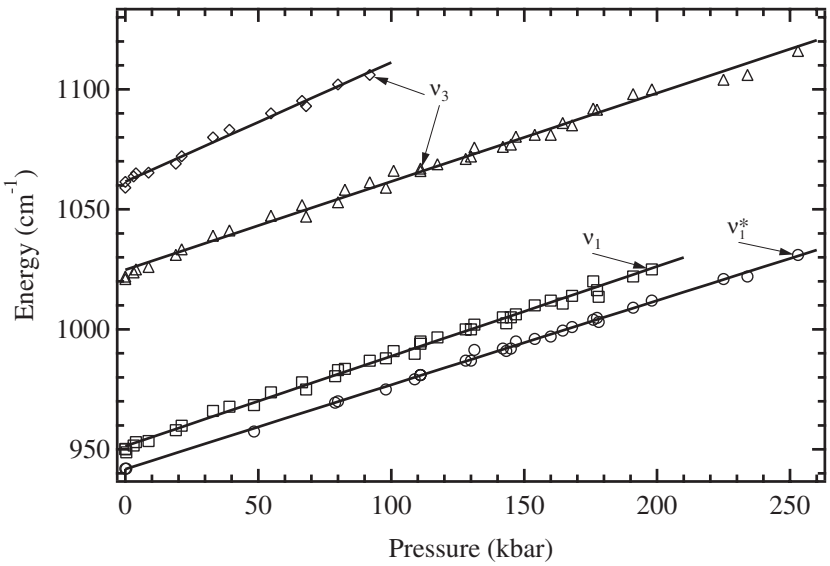

Figure 3. Pressure dependence of the stretching modes (ν_1 and ν_3) in Li_3PO_4 at room temperature. Solid lines represent linear least-squares fits of the data.

from the relative intensity of the HTP ν_1- and LTP ν_1^*-modes. An additional experiment was intentionally designed to probe the irreversibility of the phase transition. In the experiment, we first pressurized HTP Li_3PO_4 up to ∼178 kbar and found a ∼50:50 HTP:LTP phase ratio. When the pressure was released to ambient pressure, we found that the ∼50:50 HTP:LTP phase ratio remained.

Figure 3 presents the energies of the $\nu_{1,3}$-modes as a function of pressure. We obtained shift rates of 0.37(1) cm^{-1} kbar^{-1} for the HTP ν_1-mode and 0.35(1) cm^{-1} kbar^{-1} for the LTP ν_1-mode. The ν_3-mode, in both phases, also showed a similar blue-shift with pressure.

4. Luminescence spectroscopy

Mn^{5+}-doped Li_3PO_4 emits in the NIR range. Ambient-pressure 25 K luminescence spectra of Mn^{5+} are shown in figure 4(a) for HTP Mn^{5+}:Li_3PO_4 and in figure 4(b) for LTP Mn^{5+}:Li_3PO_4. Each of the spectra consisted of two strong sharp zero-phonon lines at high energy (8963 cm^{-1} (E_1) and 8980 cm^{-1} (E_2) in the HTP; 8966 cm^{-1} (E_1) and 9006 cm^{-1} (E_2) in the LTP) and weak vibronic bands at low energy. The luminescence is attributed to the $^1E \rightarrow {}^3A_2$ transition of the Mn^{5+} ion [9, 19]. The temperature dependence of the $E_{1,2}$ line intensity revealed that the E_1–E_2 splitting (17 cm^{-1} in the HTP and 40 cm^{-1} in the LTP) arises in the emitting ^1E state due to a local non-tetrahedral site distortion.

The vibronic bands are attributed to vibronic transitions associated with the bending mode (ν_2) and the stretching mode (ν_1) of $(MnO_4)^{3-}$ in Li_3PO_4 [9]. The ambient-pressure energies of the $(MnO_4)^{3-}$ $\nu_{1,2}$-modes are presented in table 1. For comparison, the data for four vibrations of the free $(MnO_4)^{3-}$ ion are also included in table 1. We note from figure 4 that the vibronic transitions in LTP Mn^{5+}:Li_3PO_4 are stronger than those in HTP Mn^{5+}:Li_3PO_4 and that the vibronic transition associated with the bending mode is stronger than that associated with the stretching mode in both phases.

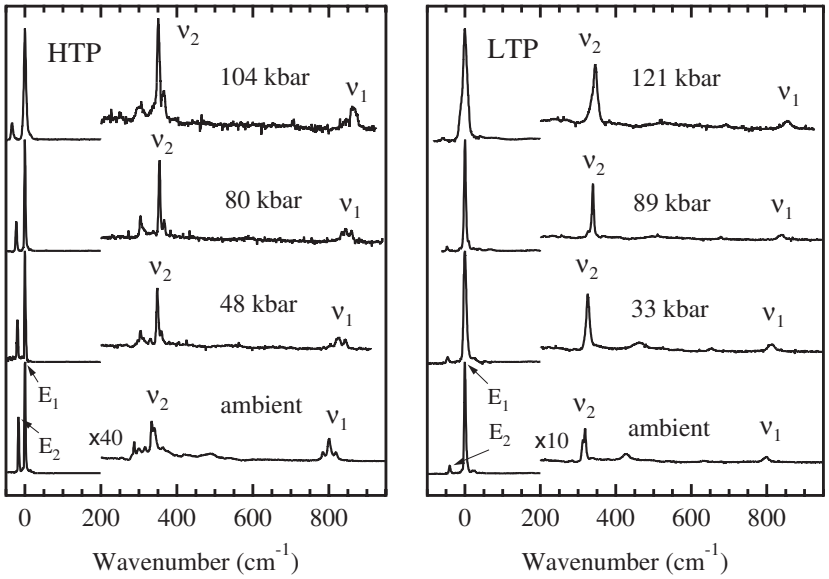

Figure 4. Ambient- and high-pressure 25 K luminescence spectra of Mn^{5+} in HTP Li_3PO_4 (left) and HTP Li_3PO_4 (right) upon excitation at $\lambda_{ex} =\sim 600$ nm. All vibronic spectra were normalized to the E_1 line intensity and scaled relative to the E_1 line energy.

Upon application of pressure, we observed a red-shift in the barycentre energy of the ^1E state and an increase in the splitting of the ^1E state (figure 5(a)). A discussion of the effect of pressure on the barycentre energy and the splitting of the ^1E state was given in our previous study [19]. Representative vibronic luminescence spectra at several pressures are shown in figure 4 relative to the energy of the E_1 line. An obvious increase in intensity of the vibronic ν_2-transition with pressure was observed in both phases. The energies of the bending mode ν_2 and stretching mode ν_1, as a function of pressure, were derived from the vibronic luminescence spectra (figure 4) and are shown in figures 5(b) and (c). In both phases, the stretching mode ν_1 exhibited a linear blue-shift with pressure (0.39(2) cm^{-1} $kbar^{-1}$ in the LTP and 0.54(3) cm^{-1} $kbar^{-1}$ in the HTP) and the bending mode ν_2 exhibited a weaker sublinear blue-shift with pressure (approximately 0.19 cm^{-1} $kbar^{-1}$ in the LTP and 0.22 cm^{-1} $kbar^{-1}$ in the HTP).

5. Electron–vibrational coupling

In our present Mn^{5+}:Li_3PO_4 systems, the presence of the vibronic ν_2-transition in the ^1E luminescence is indicative of a dynamic Jahn–Teller effect [24]. The emitting ^1E state of Mn^{5+} can be coupled to the bending mode $\nu_2(e)$ through an $E \otimes e$ Jahn–Teller coupling. The high intensity of the vibronic ν_2-transition relative to the vibronic ν_1-transition is further evidence of the presence of the $E \otimes e$ Jahn–Teller coupling in the ^1E state of Mn^{5+}.

Such a Jahn–Teller effect can be expected to enhance mixing between the ^1E state and the ^3E orbital component of the highly excited $^3T_2$ state through spin–orbit coupling. In a more distorted $(MnO_4)^{3-}$ system, we can expect a stronger vibronic ν_2-transition because of the smaller energetic separation between the ^1E state and the lowest orbital component of the excited $^3T_2$ state. This smaller separation increases the $E \otimes e$ Jahn–Teller effect

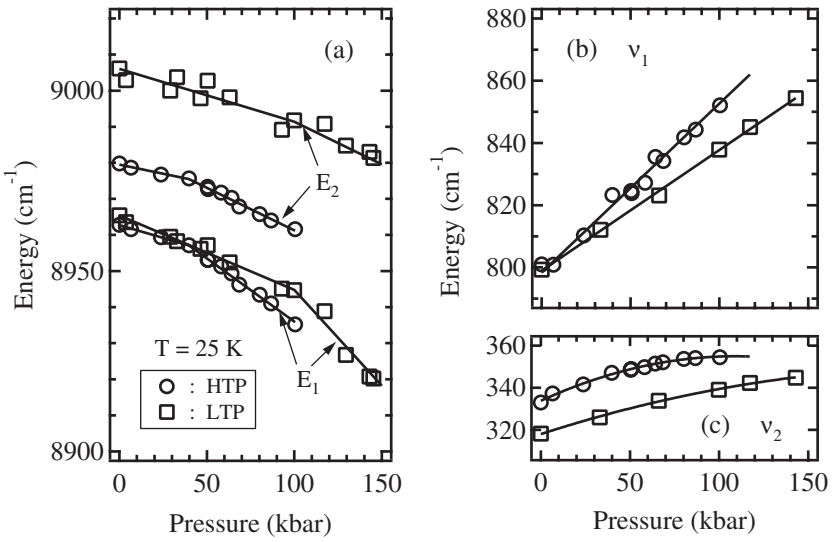

Figure 5. Energies of the $E_{1,2}$ zero-phonon lines and the bending and stretching modes ($\nu_{1,2}$) in HTP and LTP Mn^{5+}:Li_3PO_4, as a function of pressure. The solid curves are provided only as a guide to the eye.

through the spin–orbit coupling. Recent NIR luminescence studies of Mn^{5+} demonstrated an increased vibronic ν_2-transition intensity as the distortion of the host lattice increased from slight (Li_3BO_4, B = P, As, and V), to intermediate (apatite, $A_5(BO_4)_3Cl$; A = Ca, Sr, and Ba; B = P and V), and to strong (spodiosite, A_2BO_4Cl; A = Ca, Sr, and Ba; B = P and V) [9]. The larger ^1E splitting of Mn^{5+} in the LTP indicates that the $(MnO_4)^{3-}$ tetrahedron is more distorted in the LTP than in the HTP. We therefore expect a stronger vibronic ν_2-transition in the LTP.

In our previous high-pressure luminescence study [19], we observed an increased ^1E splitting and a decreased ^1E lifetime with pressure in both phases. These observations correspond to a pressure-induced increase in local distortions of $(MnO_4)^{3-}$. The pressure-induced increase in the intensity of the vibronic ν_2-transition is due to the increased local distortions that act to enhance the E $\otimes$ e Jahn–Teller coupling through enhanced spin–orbit mixing of the ^1E state and the lowest orbital component (^3E) of the $^3T_2$ state.

6. Compressibility

The energy (E_{ν_i}) of a vibrational mode (ν_i) as a function of the cell volume of a crystal (V) can be described by [25, 26]

$$\gamma_i = -\frac{\mathrm{d}\ln E_{\nu_i}}{\mathrm{d}\ln V} = \chi^{-1}\frac{\mathrm{d}E_{\nu_i}}{E_{\nu_i}\,\mathrm{d}P} \tag{1}$$

where γ_i is the mode Grüneisen parameter and χ is the compressibility of the crystal. This links the compressibility of the host material and the pressure dependence of the vibrational energy through the mode Grüneisen parameter.

A mode Grüneisen parameter (γ_i) depends primarily on the character of a vibrational mode. Different vibrational modes (ν_i) have their own characteristic values for γ_i. We can reasonably assume that γ_1(HTP) $\approx$ γ_1(LTP) for the $(PO_4)^{3-}$ ν_1-mode in the HTP and LTP Li_3PO_4. This is because the ν_1-mode is a totally symmetric internal stretching mode that describes a quasi-isotropic vibration and, furthermore, because the HTP and LTP Li_3PO_4 are dimorphic and the

Table 2. Ambient-pressure energies (cm^{-1}), absolute shifts (cm^{-1} $kbar^{-1}$), and relative shifts ($kbar^{-1}$) of the stretching modes ν_1 for $(PO_4)^{3-}$ and $(MnO_4)^{3-}$ in both LTP and HTP phases.

	$\nu_1(0)$ (cm^{-1})	$d\nu_1/dP$ (cm^{-1} $kbar^{-1}$)	$[1/\nu_1(0)](d\nu_1/dP)$ (10^{-4} $kbar^{-1}$)
$(PO_4)^{3-}$ (HTP)	950	0.37(1)	3.89
$(PO_4)^{3-}$ (LTP)	942	0.35(1)	3.72
$(MnO_4)^{3-}$ (HTP)	800	0.39(2)	4.88
$(MnO_4)^{3-}$ (LTP)	800	0.54(3)	6.75

P–O bond lengths of the $(PO_4)^{3-}$ group are very similar (on average, 1.546(7) Å in the LTP and 1.555(20) Å in the HTP) [21]. This assumption also holds reasonably well for the $(MnO_4)^{3-}$ ν_1-mode in both phases.

The high-pressure Raman results for the $(PO_4)^{3-}$ ν_1-mode energy (figure 3 and table 2) and the high-pressure luminescence results for the $(MnO_4)^{3-}$ ν_1-mode energy (figures 5(b), (c) and table 2) provide an opportunity to predict bulk and local compressibilities using equation (1). We predict similar bulk compressibilities in the two phases (χ_B(HTP) $\approx$ χ_B(LTP)) according to γ_1(HTP) $\approx$ γ_1(LTP) for the $(PO_4)^{3-}$. We also predicted a larger local compressibility (χ_L) of the $(MnO_4)^{3-}$ in the LTP relative to the HTP (χ_L(LTP) $>$ χ_L(HTP)) according to γ_1(HTP) $\approx$ γ_1(LTP) for the $(MnO_4)^{3-}$.

In our previous high-pressure study [19], we observed a pressure-induced decrease in the Racah parameter B of Mn^{5+} in both phases of Li_3PO_4 (-1.09×10^{-2} cm^{-1} $kbar^{-1}$ in the LTP and -7.27×10^{-3} in the HTP). The Racah parameter B is a measure of the coulombic interactions between the 3d electrons of a transition metal ion and is reduced through the nephelauxetic effect when the ion is incorporated into a host lattice. Since the primary effect of hydrostatic pressure yields symmetric bond compression, the nephelauxetic effect increases with increasing pressure and B decreases with increasing pressure. A larger reduction in B corresponds to a larger compressibility. This supports our present conclusion that χ_L(LTP) $>$ χ_L(HTP).

7. Conclusions

High-pressure Raman and luminescence spectroscopy studies of undoped and Mn^{5+}-doped Li_3PO_4 have been completed to gain insight into the effect of pressure on bulk and local vibrations and the influence of the vibrations on the vibronic luminescence transitions of $3d^2$ ions. An increased intensity of the vibronic transition associated with the bending mode with increasing pressure was observed and attributed to increased E $\otimes$ e Jahn–Teller coupling. Our present high-pressure results indicate that such Jahn–Teller effects occur widely in vibronic transitions of $3d^2$ systems and exert a strong influence on the optical properties of $3d^2$ ions.

Acknowledgments

We gratefully acknowledge financial support from the US National Science Foundation through grants DMR-9629990 and DMR-0107802, and also from the Donors of the Petroleum Research Fund, administered by the American Chemistry Society. We thank Professor Hans U Güdel for kindly providing Mn^{5+}-doped HTP Li_3PO_4 single crystals and Dr Toni Riedener for his initial high-pressure luminescence measurements.

References

[1] Wu X, Yuan H, Yen W M and Aitken B G 1995 *J. Lumin.* **66+67** 285
[2] Egorysheva A V, Volkov V V, Coya C and Zaldo C 1998 *Phys. Status Solidi* b **207** 283
[3] Calistru A M, Demos S G and Alfano R R 1997 *Phys. Rev. Lett.* **78** 374
[4] Scott M A, Henderson B, Gallagher H G and Han T P J 1997 *J. Phys.: Condens. Matter* **9** 9893
[5] Deghoul F, Chermette H, Rogemond F, Moncorgé R, Stückl C and Daul C 1999 *Phys. Rev.* B **60** 2404
[6] Kück S, Petermann K, Pohlmann U and Huber G 1995 *Phys. Rev.* B **51** 17 323
Kück S, Petermann K, Pohlmann U and Huber G 1996 *J. Lumin.* **68** 1
[7] Riley M J, Krausz E R, Manson N B and Henderson B 1999 *Phys. Rev.* B **59** 1850
[8] Hazenkamp M F, Güdel H U, Atanasov M, Kesper U and Reinen D 1996 *Phys. Rev.* B **53** 2367
[9] Oetliker U, Herren M, Güdel H U, Kesper U, Albrecht C and Reinen D 1994 *J. Chem. Phys.* **100** 8656
[10] Okhrimchuk A G and Shestakov A V 2000 *Phys. Rev.* B **61** 988
[11] Brunold T, Hauser A and Güdel H U 1994 *J. Lumin.* **59** 321
[12] Hoffman K R, Casas-Gonzalez J, Jacobsen S M and Yen W M 1991 *Phys. Rev.* B **44** 12 589
[13] Buijsse B, Schmidt J, Chan I Y and Single D J 1995 *Phys. Rev.* B **51** 6215
[14] Reinen D, Rauw W, Kesper U, Atanasov M, Güdel H U, Hazenkamp M F and Oetliker U 1997 *J. Alloys Compounds* **246** 193
[15] Hömmerich U, Eilers H, Yen W M, Jia W and Wang Y 1994 *Opt. Commun.* **106** 218
[16] Shen Y R, Hömmerich U and Bray K L 1997 *Phys. Rev.* B **56** R473
[17] Shen Y R and Bray K L 2000 *Phys. Rev. Lett.* **84** 3990
[18] Shen Y R, Riedener T and Bray K L 2000 *Phys. Rev.* B **61** 9277
[19] Riedener T, Shen Y R, Smith R J and Bray K L 2000 *Chem. Phys. Lett.* **321** 445
[20] Zemann V J 1960 *Acta Crystallogr.* **13** 863
[21] Keffer C, Mighell A, Mauer F, Swanson H and Block S 1967 *Inorg. Chem.* **6** 119
[22] Jayaraman A 1986 *Rev. Sci. Instrum.* **57** 1013
[23] Gonzalez-Vilchez F and Griffith W P 1972 *J. Chem. Soc. Dalton Trans.* 1416
[24] Ballhausen C 1988 *Vibronic Processes in Inorganic Chemistry (NATO ASI Series, vol 288)* ed C D Flint (Dordrecht: Kluwer) p 53
[25] Sherman W F and Wilkinson G R 1980 *Advances in Infrared and Raman Spectroscopy* vol 6, ed R J H Clark and R E Hesler (London: Heyden) pp 158–336
[26] Ferraro J R 1988 *Vibrational Spectroscopy at High External Pressures* (New York: Academic)